The Journal of Experimental Biology 202, 1195–1203 (1999)
Printed in Great Britain © The Company of Biologists Limited 1999
JEB2086

PREY CAPTURE IN THE WEAKLY ELECTRIC FISH *APTERONOTUS ALBIFRONS*: SENSORY ACQUISITION STRATEGIES AND ELECTROSENSORY CONSEQUENCES

MARK E. NELSON[1,2,3,*] AND MALCOLM A. MACIVER[2,3]

[1]*Department of Molecular and Integrative Physiology,* [2]*The Neuroscience Program* and [3]*The Beckman Institute for Advanced Science and Technology, University of Illinois at Urbana-Champaign, Urbana, IL 61801, USA*

*e-mail: m-nelson@uiuc.edu

Accepted 25 January; published on WWW 21 April 1999

Summary

Sensory systems are faced with the task of extracting behaviorally relevant information from complex sensory environments. In general, sensory acquisition involves two aspects: the control of peripheral sensory surfaces to improve signal reception and the subsequent neural filtering of incoming sensory signals to extract and enhance signals of interest. The electrosensory system of weakly electric fish provides a good model system for studying both these aspects of sensory acquisition. On the basis of infrared video recordings of black ghost knifefish (*Apteronotus albifrons*) feeding on small prey (*Daphnia magna*) in the dark, we reconstruct three-dimensional movement trajectories of the fish and prey. We combine the reconstructed trajectory information with models of peripheral electric image formation and primary electrosensory afferent response dynamics to estimate the spatiotemporal patterns of transdermal potential change and afferent activation that occur during prey-capture behavior. We characterize the behavioral strategies used by the fish, with emphasis on the functional importance of the dorsal edge in prey capture behavior, and we analyze the electrosensory consequences. In particular, we find that the high-pass filter characteristics of P-type afferent response dynamics can serve as a predictive filter for estimating the future position of the prey as the electrosensory image moves across the receptor array.

Key words: prey capture, *Apteronotus albifrons*, P-type afferent, electrolocation, signal processing, computational neuroethology.

Introduction

All animals are faced with the challenging task of extracting useful information about their environment from the barrage of sensory stimuli impinging on their receptor surfaces. To address this challenge, animals use a variety of strategies for actively positioning their receptor surfaces and for adjusting their neural processing to optimize the content and quality of incoming signals. Research into the control of sensory acquisition requires a neuroethological perspective that takes into account both behavioral and neural aspects of the problem. At the behavioral level, it is important to understand how movements generated by the animal during sensory acquisition influence the incoming data stream. At the neural level, it is important to understand how subsequent processing of this data stream by the nervous system allows the animal to extract and enhance signals of behavioral relevance.

Weakly electric fish provide a useful model system for studies of sensory acquisition (for reviews, see Bastian, 1986, 1995). The black ghost knifefish *Apteronotus albifrons* is a gymnotiform weakly electric fish with a long flattened trunk containing an electric organ that generates a continuous wave-type electric organ discharge (EOD). The EOD is high-frequency (approximately 1 kHz) and low-amplitude (approximately 1 mV cm^{-1} near the fish) (Knudsen, 1975). This fish is a nocturnal hunter that feeds predominantly on insect larvae and small crustaceans in the freshwater rivers of South America (Hagedorn, 1986; Winemiller and Adite, 1997). Since these prey differ in electrical impedance from the surrounding water, they give rise to small perturbations in the electric field around the fish. These perturbations in turn give rise to slight changes in the potential difference across the skin of the fish, which are transduced by extremely sensitive electroreceptor organs in the skin.

Electroreceptor organs, which are distributed over the entire body surface of the fish, can be classified into two major classes. Tuberous electroreceptor organs are specialized for detecting modulations of the high-frequency self-generated electric field (often referred to as the ‘active’ electrosense). A second class, called ampullary organs, is specialized for detecting low-frequency electric fields arising from external sources such as the bioelectric fields generated by other aquatic organisms (the ‘passive’ electrosense). In addition to the active and passive electrosensory systems, the fish also has a mechanosensory lateral line system. All three of these related octavolateral systems can potentially provide information that may aid the fish when hunting for prey at night or in muddy water (Hoekstra and Janssen, 1986; Kirk, 1985; Montgomery,

1989; Peters and Bretschneider, 1972). This paper, however, will focus on contributions of the active electric sense.

In addition to having remarkable sensory capabilities, black ghost knifefish also have an unusual locomotor system which allows them to swim forwards, backwards and sideways and to hover. Propulsive forces are generated by undulations of a long ribbon fin that runs most of the length of the ventral body surface. During locomotion, the trunk of the fish remains relatively rigid and 'knifelike' as the fish slices through the water. Because the control of the trunk musculature is independent of the control of the ribbon fin, the fish has considerable freedom in how it orients its body, and hence its electroreceptor array and electric organ, as it moves through the water. It has been suggested that this gymnotiform mode of swimming provides a high degree of maneuverability and is well suited to foraging in complex environments (Blake, 1983). The body of the weakly electric fish can be thought of as a dynamic sensory antenna that can be repositioned to improve the reception of signals of interest from the environment. This functionality as a sensory antenna is similar to that proposed for the paddlefish rostrum (Wilkens et al., 1997) and the platypus bill (Scheich et al., 1986), which are extended peripheral sensory structures used for prey detection *via* the passive electric sense.

By controlling the position, velocity and orientation of their body during prey capture, fish can actively influence the spatiotemporal patterns of incoming electrosensory signals. While there is evidence that the active electric sense can contribute to prey detection and localization in weakly electric fish (Lannoo and Lannoo, 1993; von der Emde, 1994; von der Emde and Bleckmann, 1998), there is little quantitative information available about the positioning of the electrosensory array during prey-capture behavior. In this paper, we extend earlier preliminary studies on this subject (MacIver et al., 1996; MacIver and Nelson, 1997) by using an improved analysis methodology to extract quantitative information on fish position, orientation and velocity during prey capture. We subsequently use this information to reconstruct electrosensory image sequences. The overall goal of these studies is to quantify the behavioral aspects of sensory acquisition in *Apteronotus albifrons* and to understand the electrosensory consequences of observed movements.

Materials and methods

Animals

Adult weakly electric fish of the species *Apteronotus albifrons* (black ghost knifefish), 14–18 cm in length, were used in this study. Fish were maintained on a 12 h:12 h light:dark cycle at a temperature of 26±1.0 °C in water with a conductivity of 300±10 μS cm^{-1} and a pH of 7.0±0.1. Prey were mature *Daphnia magna* (water fleas) 2–3 mm in length.

Behavioral data acquisition

Fish were housed in a rectangular Plexiglas aquarium with a central area partitioned from the rest of the tank to form a behavioral arena (40 cm×30 cm×20 cm). The central arena was imaged by two video cameras which provided top and side views, allowing three-dimensional reconstruction of behavioral trajectories (Fig. 1A). Video signals from the two cameras were electronically merged and recorded onto video tape for subsequent analysis. The video sampling rate was 60 frames s^{-1}, where a frame is defined as one video field with the alternate scan lines interpolated. To eliminate visual cues, prey-capture behavior was observed under infrared (880 nm) illumination provided by high-intensity infrared diodes. The illuminators, cameras and aquarium were housed within a light-tight enclosure. Four fish were held in individual holding bays electrically insulated from the central arena; one fish at a time was allowed into the recording arena through a Plexiglas door. A long narrow tube was used to introduce prey one at a time into the aquarium without introducing visible light and with minimal mechanical disturbance. Prey-capture behavior was observed during the first 3 h of the dark portion of the light/dark cycle. Video-taped recordings of prey-capture behavior were visually scanned offline to identify segments to be digitized for further analysis. Segment selection was based on three criteria: (1) a successful capture, or an unsuccessful capture with a lunge or an abrupt change in swimming pattern near the prey; (2) fish and prey visible in both views except for brief occlusions; (3) prey at least 2 cm from the bottom and sides of the tank.

Trajectory analysis

For each frame in the sequence, a computer-generated wireframe model of the fish with 90 total vertices was interactively overlaid on the digitized video image of the fish to determine the body position and geometry (Fig. 1B). The wireframe fish model was derived from a urethane cast of *A. albifrons* digitized using a three-dimensional stylus-type digitizer (MicroScribe, Immersion Co). The interactive video overlay procedure yielded eight parameter values per frame: three position coordinates (x, y, z) corresponding to the location of the tip of the snout, three angular coordinates (roll, pitch, yaw) corresponding to the rigid body orientation of the fish in the tank, and two bend parameters (dorsal–ventral and lateral) corresponding to the non-rigid degrees of freedom. A single point in each view was used to mark the center of the prey (Fig. 1B). All data analysis procedures were carried out using MATLAB (The MathWorks) running on a Sun workstation.

Electrosensory image reconstruction

On the basis of reconstructed trajectories, we computed the spatial distribution and time course of transdermal voltage changes on the skin. Electrosensory images were computed by modeling the prey as an ideal spherical conductor with a diameter of 3 mm. The dipolar field perturbation $\delta\phi(\mathbf{r})$ of a perfectly conducting sphere is given by Rasnow (1996) as:

$$\delta\phi(\mathbf{r}) = \left(\frac{a^3}{|\mathbf{r}|^3}\right)(\mathbf{E_{fish}} \cdot \mathbf{r}), \quad (1)$$

where a is the radius of the sphere, $\mathbf{r}$ is a vector from the center

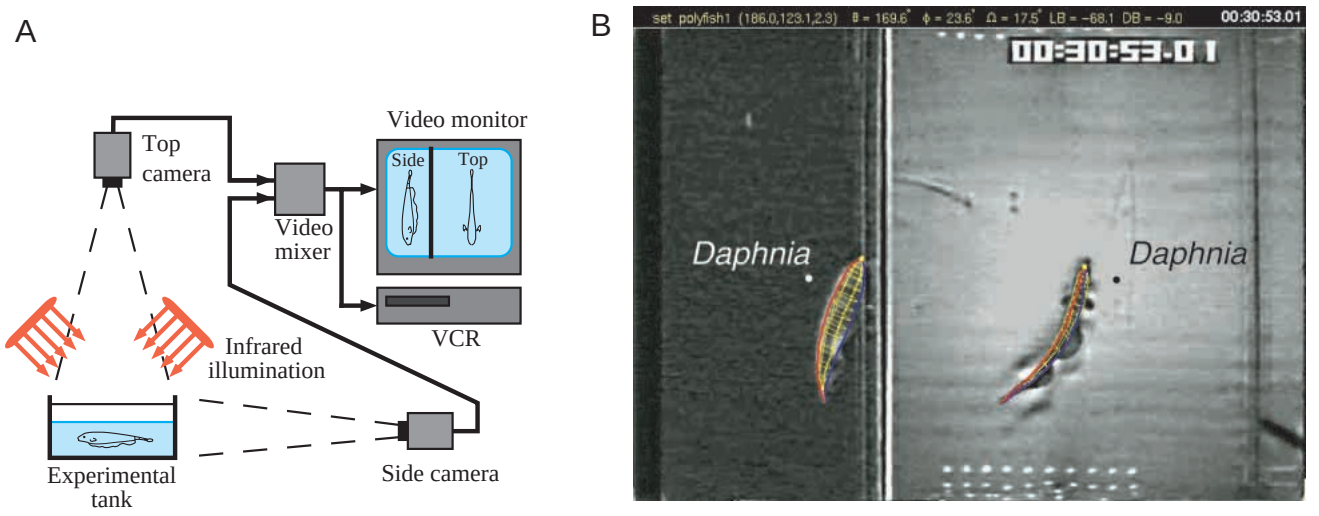

Fig. 1. Behavioral recording arrangement and trajectory reconstruction. (A) Schematic diagram of the two-camera infrared video apparatus. (B) Digitized video image showing both the side (left) and top (right) views of the fish in the experimental tank. During offline analysis, a wireframe mesh model (shown in color) is interactively superimposed on the digitized images in the prey-capture sequence to determine the position, angular orientation and bend parameters of the fish. A small dot is used to mark the location of the prey.

of the sphere to the receptor surface, and $\mathbf{E}_{\mathbf{fish}}$ is the electric field vector at the location of the sphere. Equation 1 is the limiting case of a more general formula involving both prey and water resistivity; the resistivity terms drop out of the general equation when considering a perfect conductor. The terms involving resistivity contribute an overall scaling factor, but do not alter the spatial structure of the dipole field. Because actual prey are not perfect conductors, this approximation overestimates the magnitude of the voltage change and therefore provides an upper limit to the size of the perturbation. Computing the spatial profile of the electrosensory image for each frame involves evaluating equation 1 for fixed values of $\mathbf{E}_{\mathbf{fish}}$ and a and with $\mathbf{r}$ corresponding to all points on the electroreceptor surface; computing the temporal profile involves repeating this procedure for all frames in the sequence.

P-type electrosensory afferent response dynamics

There are two physiologically defined classes of tuberous electrosensory afferents. Probability-coding (P-type) afferents encode changes in the amplitude of the transdermal potential, while time-coding (T-type) afferents encode changes in the timing of the zero-crossing of the transdermal waveform (Scheich et al., 1973). P-type afferents allow the fish to detect objects that have an electrical impedance that differs from that of the surrounding water (Bastian, 1981). T-type afferents allow the fish to detect phase shifts associated with the capacitative component of the impedance, which may be useful for distinguishing animate from inanimate objects (see von der Emde, 1999; this issue). In the present paper, we focus on the contribution of P-type afferents, which are far more numerous than T-type afferents in *Apteronotus*. In apteronotids, almost all the tuberous afferents in the head and trunk region are P-type and are thus likely to dominate the tuberous electrosensory component of detection and localization. T-type units are found primarily on a specialized sensory structure called the dorsal filament (Franchina and Hopkins, 1996) and may contribute to detection and discrimination in some circumstances (see Discussion).

We estimate changes in P-type electrosensory afferent firing rate on the basis of an empirically derived model of afferent response dynamics (Nelson et al., 1997). The transdermal potential changes described above serve as input to the model. The afferent model is a linear–nonlinear cascade model consisting of a second-order linear model that describes the frequency-dependence of the gain and phase of the response, in series with a static nonlinearity that incorporates the effects of firing rate rectification and saturation. The second-order model has a transfer function $H(s)$ given by:

$$H(s) = \frac{G_a s}{s + 1/\tau_a} + \frac{G_b s}{s + 1/\tau_b} + G_c \,, \qquad (2)$$

where s is the complex frequency, G_a–G_c are gain terms and τ_a and τ_b are time constants. Parameter values for the model were G_a=11 300 spikes s^{-1} mV^{-1}, G_b=370 spikes s^{-1} mV^{-1}, G_c=630 spikes s^{-1} mV^{-1}, τ_a=0.0029 s and τ_b=0.318 s. This model accurately describes the experimentally measured frequency response characteristics of P-type afferents in the closely related species *Apteronotus leptorhynchus* over a range of amplitude-modulated frequencies from 0.1 to 200 Hz (Nelson et al., 1997). All statistical measures below are reported as mean±S.D.

Results

Time of detection

We selected 25 prey-capture sequences for reconstruction

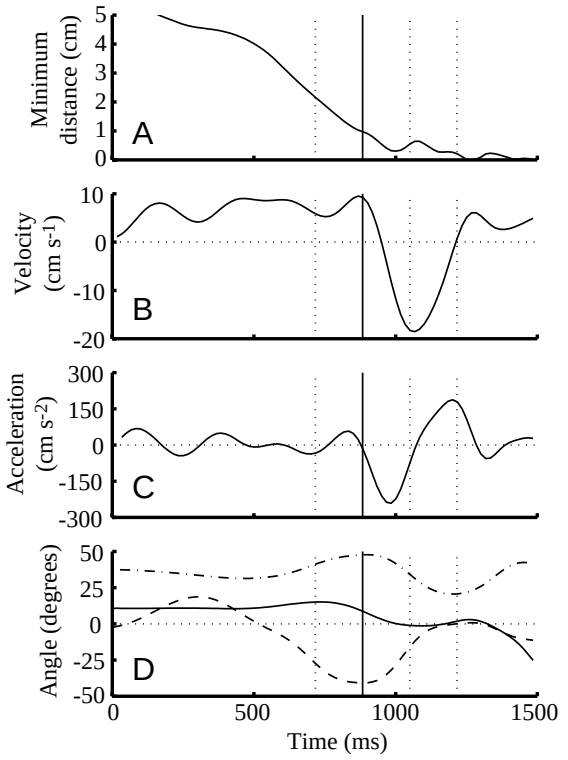

Fig. 2. Time course of trajectory parameters for a representative prey-capture sequence. Vertical lines indicate the times corresponding to the snapshots of this sequence shown in Fig. 4; the solid vertical line indicates the estimated time of detection, while dotted vertical lines indicate times of the pre- and post-detection snapshots. Prey capture (ingestion) occurs at the maximum time value shown on the abscissa (t=1500 ms). (A) Minimum distance from the prey to the body surface; (B) longitudinal velocity of the fish; (C) longitudinal acceleration of the fish; (D) body roll (solid line), body pitch (dash-dot line) and lateral tail bend angle (dashed line).

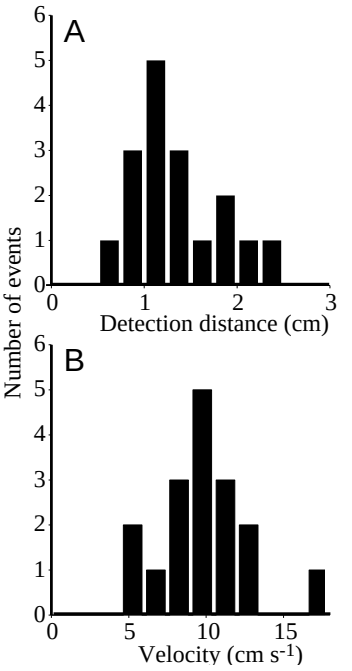

Fig. 3. (A) Detection distance distribution for 17 prey-capture events summarizing the minimum distance between the prey and the body surface at the time of detection (mean value 1.2±0.5 cm). (B) Relative longitudinal velocity between the fish and prey at the time of detection (mean value 9.2±3.0 cm s^{-1}; mean ± S.D.).

on the basis of the selection criteria outlined above. In 21 of 25 cases, the fish was initially swimming forward with a mean longitudinal velocity of 7.1±4.0 cm s^{-1}. In four cases, the fish was initially swimming backwards with a mean longitudinal velocity of −14±7.3 cm s^{-1}. For the 21 forward-swimming cases, we always observed a reversal in swimming direction prior to prey capture. The longitudinal velocity reversed from an average of +7.1±4.0 cm s^{-1} (N=21) to a peak negative velocity of −17±5.8 cm s^{-1} (N=21). For 17 of these 21 forward-swimming sequences, the onset of reverse swimming was unimodal and sufficiently abrupt to allow us accurately to determine a time of onset; the mean time to reach peak negative velocity was 370±150 ms (N=17) with a peak deceleration of −210±68 cm s^{-2} (N=17). We refer to these rapid reversals from forward to backward swimming as ‘reverse thrusts’. During a reverse thrust, the fish typically moves backwards approximately one-fifth (21±13 %, N=17) of its total body length prior to capturing the prey. Longitudinal velocity and acceleration profiles for a typical reverse thrust trajectory are shown in Fig. 2B,C. Reverse thrusts were observed only in response to potential prey; changes in swimming direction that occurred at other times were more gradual, with lower peak accelerations.

We use the onset of the reverse thrust, as indicated by the negative-going zero-crossing of longitudinal acceleration, as an estimate of the putative time of prey detection. Subsequent results and analysis in this paper will be confined to those sequences in which a detection time could be accurately established. For these 17 sequences, the mean distance from the prey to the closest point on the body surface at the time of detection was 1.2±0.5 cm (N=17). The distribution of detection distances is shown in Fig. 3A. The mean longitudinal velocity at the time of detection was 9.2±3.0 cm s^{-1} (N=17); the corresponding velocity distribution is shown in Fig. 3B. As described below, combined measurements of distance and velocity allow us to estimate both the spatial and temporal characteristics of the electrosensory image projected onto the receptor surface at the time of prey detection.

Search phase (pre-detection)

Having established a putative time of detection, we analyzed the movement trajectories of the fish during the pre- and post-detection phases of the behavior. During the pre-detection phase, the fish searches the tank for potential targets. In the calm water conditions used here, *Daphnia* moved relatively slowly in the tank. At the time of detection, the average *Daphnia* velocity was 2.4±1.9 cm s^{-1} (N=17) compared with an average fish velocity of 11.4±2.8 cm s^{-1} (N=17). Thus, a

successful detection under these conditions typically involved a relatively rapidly moving fish running into a slowly moving *Daphnia*. Search trajectories tended to cover the entire volume of the tank using combinations of forward swimming, backward swimming and side-scanning movements. Analysis of midtank search trajectories with no prey in the tank revealed that fish spent approximately 50 % of the time in forward swimming, 25 % in backward swimming and 25 % in side-scanning movements. Reverse swimming and side scanning were more common near the edges of the tank.

While swimming forward searching for prey, the fish tended to maintain an upright posture (roll angle −3±13 °, N=17) with the head angled downwards (pitch angle 26±14 °, N=17). This swimming posture resulted in the dorsal surface of the fish forming the leading edge as the fish moved through the water. The body of the fish was generally straight with little lateral tail bend, except when the fish was executing turns to change heading direction. During turns, which were often linked together in alternating left–right sequences, the degree of tail bend was significant. Fig. 2D shows values for roll, pitch and lateral tail bend during a representative prey-capture sequence.

Scan and intercept phase (post-detection)

Once the fish had detected the prey, it initiated a reverse thrust that brought its mouth within a few millimeters of the prey. We refer to this post-detection phase of the behavior as the ‘scan and intercept’ phase, reflecting the observation that during the reversal the fish appears to scan the prey across its sensory array before intercepting it with the mouth. Interception involved a short (a few millimeters) forward or side lunge to ingest the prey using a suction mechanism (Lannoo and Lannoo, 1993). Reverse thrusts were accompanied by subtle shifts in body posture that generally brought the prey closer to the electroreceptor surface (Fig. 2A). During the reverse scan, the magnitude of the roll angle tended to increase, taking the fish from a relatively upright posture at the time of detection into a final posture in which the body had rolled left or right by a significant amount (40 ° root mean square, RMS). During the scan phase, the pitch angle tended to decrease, bringing the fish closer to the horizontal plane containing the prey. Also, we observed that if the tail was initially bent at the time of detection, the degree of tail bend tended to decrease during the reverse scan such that the fish was nearly straight before it executed the final forward or sideways lunge to capture the prey.

Electrosensory image characteristics

We computed the spatial and temporal patterns of the electrosensory image intensity on the receptor surface using equation 1 and the reconstructed fish and prey trajectories. Fig. 4A shows the resulting patterns of transdermal potential change at four time points (vertical lines in Fig. 2) during a representative prey-capture sequence. These images represent the instantaneous electric image at the peak of the electric organ discharge (EOD) cycle. Time runs vertically from bottom to top in the figure. At the beginning of the sequence (167 ms before prey detection), the prey is located approximately 2 cm above the dorsum and slightly to the left of the fish. The fish is swimming forwards with its head pitched downwards, a slight leftward body roll and a lateral tail bend to the left (for quantitative values, see Fig. 2). In the next snapshot (at the time of prey detection), the fish begins a reverse thrust to change its swimming direction. The prey is approximately 1 cm from the receptor surface, and the electrosensory image is nearly centered on the dorsal midline; the electrosensory image is weak and diffuse. In the third snapshot (167 ms after detection), the fish has reached its peak negative velocity. The prey is now approximately 0.4 cm from the receptor array; the electrosensory image is much stronger and more focal. The final snapshot (333 ms after detection) is near the end of the reverse thrust when the fish is about to make a final lunge at the prey. At this point, the prey is approximately 0.25 cm above the receptor surface. Quantitative values for the peak amplitude, spatial bandwidth and temporal bandwidth of the electrosensory image are provided in Table 1.

Predicted P-type electrosensory afferent responses

Using the reconstructed changes in transdermal potential shown in Fig. 4A, we computed the corresponding change in P-type electrosensory afferent firing rate on the basis of the model of afferent response dynamics described by equation 2. Fig. 4B shows the estimated changes in P-unit firing rate corresponding to the changes in transdermal potential shown in Fig. 4A. Note that the change in transdermal potential in Fig. 4A is unimodal, whereas the change in afferent firing rate in Fig. 4B is typically bimodal. Primary afferents typically show

Table 1. *Trajectory parameters and estimated electrosensory image properties for the prey-capture snapshots shown in Fig. 4*

Time relative to detection (ms)	Minimum distance to prey (cm)	Relative velocity (cm s^{-1})	Peak transdermal change (μV RMS)	Spatial bandwidth (cycles cm^{-1})	Temporal bandwidth (cycle s^{-1})	Peak afferent change (spikes s^{-1})
−167	2.3	5.5	0.6	0.2	1.1	1.4
0	1.0	9.0	3.2	0.5	4.5	7.0
+167	0.42	−19.0	18.0	1.2	23.0	48.0
+333	0.26	0.6	49.0	1.9	1.1	120.0

RMS, root mean square.

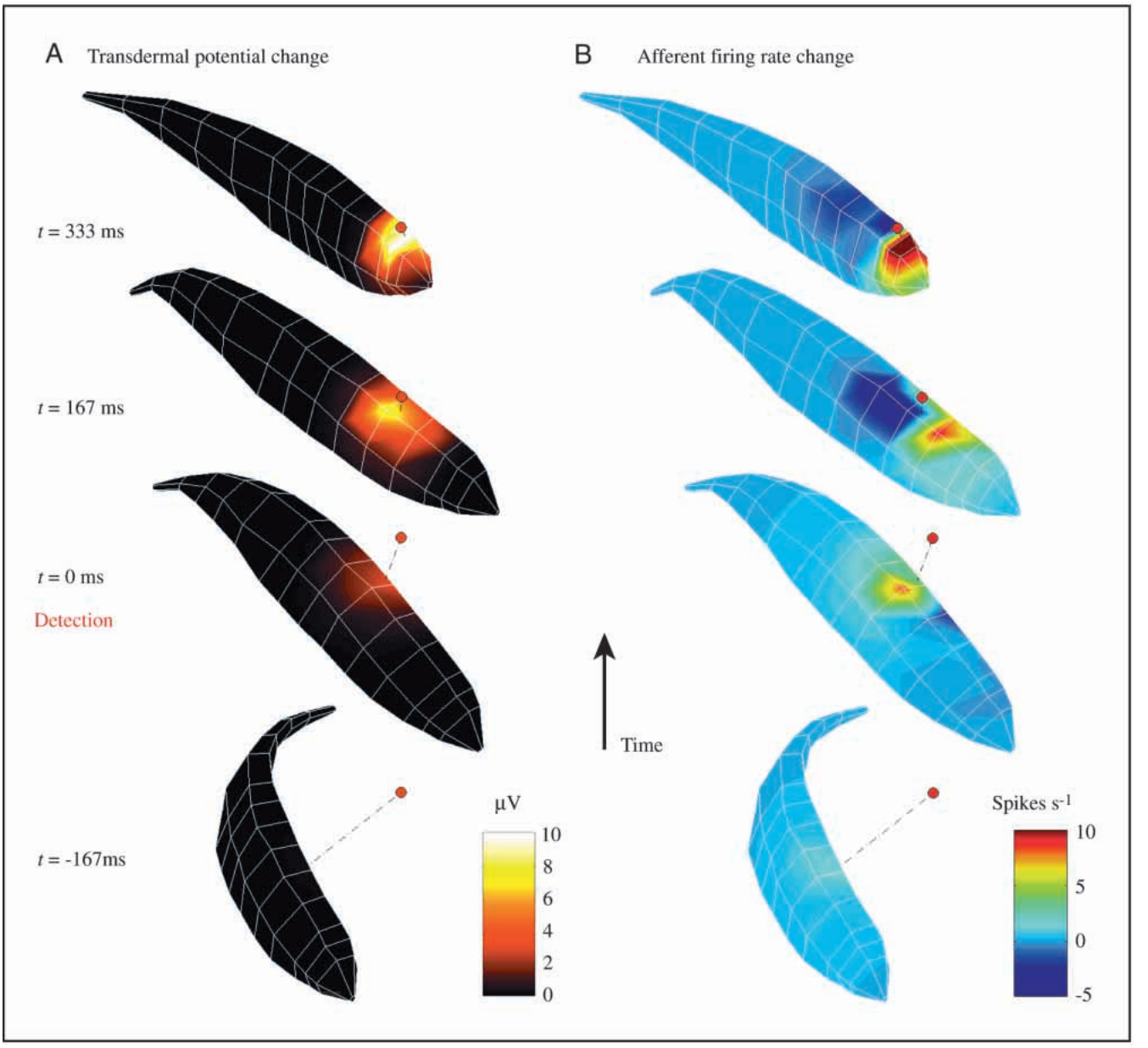

Fig. 4. Selected 'snapshots' showing the three-dimensional geometry and electrosensory images at four time points during a representative prey-capture sequence. Time (in ms) runs vertically from bottom to top; time values are measured relative to prey detection (t=0). Corresponding time points are indicated by vertical lines in Fig. 2. (A) Change in transdermal potential (in μV). (B) Change in firing rate (in spikes s^{-1}) of P-type electrosensory afferent nerve fibers. Quantitative values for selected trajectory parameters and electrosensory image characteristics are given in Table 1.

two regions of firing rate change: a region ahead of the peak in transdermal potential showing an increase in activity, and a trailing region behind the peak showing a decrease in activity. Quantitative values for the peak change in afferent firing rate are provided in Table 1. The implications of this spatial pattern of afferent activity will be discussed below.

Discussion

Black ghost knifefish are remarkably agile swimmers. They swim both forwards and backwards through a range of velocities and orientations, from right-side-up to up-side-down, from horizontal side-searching movements across the bottom of the tank to vertical sweeps around the edges of the tank with their snout at the water surface. By virtue of their knifelike body geometry and unique ribbon-fin propulsion system, they can rapidly change swimming speeds and direction or can hover for extended periods in an almost stationary position.

Pre-detection strategies

Despite all the degrees of freedom in their locomotor

repertoire, one consistent feature of the swimming patterns we observed during prey-search behavior is that the dorsal surface of the fish typically forms the leading edge as the fish moves through the water. Although the fish sometimes swam straight ahead or straight back, we observed more commonly that the fish tended to swim with an appreciable body pitch, such that the dorsum of the fish formed the leading surface. For forward swimming in a normal upright posture, this means that the head is pitched downwards, while for reverse swimming the head is pitched upwards. Side-scanning movements in which the velocity vector is roughly orthogonal to the long axis of the fish were always with the dorsal edge leading and were never laterally or ventrally directed.

In terms of prey detection efficiency, the strategy of leading with the dorsal edge is presumably more effective than straight-ahead swimming because by pitching the body the fish is able to use trunk receptors to increase the effective search volume as it moves through the water. Straight-ahead swimming, in either the forward or reverse direction, would result in trunk receptors passing through the same volume as the head receptors, thus providing little additional information to the animal. In addition to increasing the search efficiency, leading with the dorsal edge has several other possible advantages from a sensory acquisition standpoint.

First, the electroreceptor density is considerably higher along the dorsal edge than on other parts of the trunk. Carr et al. (1982) found that the tuberous electroreceptor organ density on the dorsal surface of the trunk is a factor of 2–3 times higher than on the ventral and lateral surfaces. Thus, the dorsal edge should be the most sensitive portion of the trunk for detecting weak electrosensory signals.

Second, because of biomechanical and hydrodynamic constraints, it is easier for the fish to approach the prey with the dorsal edge than to move laterally to reduce the distance between the prey and the receptor surface. Despite their highly maneuverable design, it is virtually impossible for knifefish to execute pure lateral translations, both because they cannot generate appropriately directed propulsive forces with their fins and because the hydrodynamic reaction forces are unfavorable. In contrast, dorsally directed translations can be executed with relative ease. Thus, it is easier for the fish to maneuver the receptor surface closer to the prey when the prey lies in the dorsal quadrant than when the prey is positioned laterally or ventrally to the fish.

Third, fish in the family Apteronotidae possess a specialized sensory structure on the dorsal midline known as the dorsal filament (Franchina and Hopkins, 1996). In *A. albifrons*, this filament runs along the caudal-most third of the dorsum. The dorsal filament is covered with hundreds of tuberous electroreceptors, most of which appear to be phase-coding T-units on the basis of their morphology. The vast majority of tuberous electroreceptors on other portions of the trunk are amplitude-coding P-units; thus, the dorsal filament may be a specialized sensory structure aiding in sensory discrimination of potential targets on the basis of their complex impedance characteristics.

Fourth, bringing the prey along the dorsal midline may facilitate spatial localization by allowing comparisons between receptor activation on the left and right sides of the body. While there is no direct evidence to support this hypothesis, one possible computational strategy for determining the elevation of the prey relative to the fish's body axis would be to compare the signal strength between the two sides of the body. A balanced stimulus would indicate a prey location directly above the dorsal midline, while an imbalance could serve as a relative measure of the angular deviation from the dorsal plane. Because of the bilateral symmetry of the animal, such comparisons are feasible along the dorsal midline. In contrast, a similar computational strategy would be difficult to implement along the lateral midline because of asymmetries in body geometry and receptor density along the dorsal–ventral axis.

Post-detection strategies

Once the prey had been detected, the post-detection behavior consisted of a reverse scan followed by a short lunge to capture the prey. The duration of the reverse scan, from the time of detection to the time of capture, is typically between 300 and 800 ms, with shorter times for prey detected near the head and longer times for prey near the tail. In almost all scan sequences, the minimum distance between the prey and the receptor surface tended to decrease steadily throughout the duration of the scan. Thus, an important component of the post-detection strategy is to adjust the body posture and orientation in such a way as to close the gap between the prey and the receptor surface during the reverse scan. The manner in which this is accomplished is highly variable because the post-detection trajectories are dependent on both the initial location of the prey and the initial body posture of the fish at the time of prey detection. For prey detected near the dorsal midline, the scan trajectory usually maintained the electrosensory image on the dorsal edge until it reached the head, at which point it dropped down the side of the head towards the mouth. In several cases where the initial electrosensory image was on the trunk, but off the dorsal midline, the fish executed a body roll during the scan to bring the image along the dorsal surface. However, when the initial image was near the head, but off the dorsal midline, the scan trajectory was often a direct path towards the mouth.

Electrosensory consequences

Having reconstructed the changes in transdermal potential and corresponding changes in P-type afferent firing rate during prey-capture behavior, we now have access to a detailed quantitative description of the active electrosensory data stream from which the fish can extract information about its environment. At the time of prey detection, the upper limit on the RMS change in peak transdermal potential is estimated to be a few microvolts (see Table 1). This value is to be compared with a nominal RMS transdermal voltage that is of the order of 1 mV. Thus, the transdermal potential profile at the time of detection has a peak value that is at most a few tenths of a per cent of the baseline level. Recall that we have computed the

electrosensory image under the most favorable of assumptions, namely that the prey is a perfect conductor. More realistic values for prey impedance would decrease the electrosensory image amplitude even further. The spatial profile of the transdermal potential at the time of detection has a full-width at half-maximum (FWHM) of approximately 1 cm. The density of tuberous electroreceptors on the trunk is approximately 3 mm^{-2} (Carr et al., 1982), so there would be approximately 200 electroreceptors within a circular region with a diameter of 1 cm corresponding to the FHWM of the image. When transformed into the frequency domain, this electrosensory image has a spatial bandwidth of approximately 0.5 cycles cm^{-1}.

Given a typical velocity difference (relative velocity) of 9 cm s^{-1} between the fish and prey at the time of detection, a spatial bandwidth of 0.5 cycles cm^{-1} corresponds to a temporal bandwidth of 4.5 cycles s^{-1}. This represents the bandwidth of the amplitude modulation (AM) signal that will be transduced by P-type electrosensory afferents. As shown in Table 1, the temporal bandwidth of the electrosensory image increases to approximately 25 Hz shortly after detection. This increase is due to the rapid increase in relative velocity during the reverse thrust and to the increase in spatial bandwidth as the prey is brought closer to the receptor surface. Since P-type afferents have high-pass filter characteristics (Nelson et al., 1997), they are more sensitive to high-frequency AM signals. Hence, by increasing the temporal bandwidth of the signal, the rapid reversal may serve to improve the signal-to-noise ratio of the initially weak electrosensory signal.

At the time of detection, the estimated peak change in P-unit firing rate is 7 spikes s^{-1} (see Table 1). This change occurs on top of a baseline level of afferent firing which averages approximately 300 spikes s^{-1} (Bastian, 1981). Thus, the change in afferent firing rate at the time of detection represents a few per cent change in the baseline rate, whereas the change in transdermal potential was only a few tenths of a per cent of its baseline value. This differential sensitivity arises because P-units are phasic and respond to the rate of change of the transdermal potential rather than to its absolute value. Another effect of the high-pass filter properties is evident in the reconstructed spatial profile of afferent activity. As can be seen by comparing corresponding images in Fig. 4A and Fig. 4B, the peak of afferent activity is located ahead of the transdermal potential peak, while the negative 'after image' in the afferent activity is located behind the transdermal potential peak. As the electrosensory image moves across the receptor array, there is a positive rate of change in transdermal potential on the leading edge of the image, generating a strong excitatory response in the afferents. Conversely, a negative rate of change occurs on the trailing edge of the image, giving rise to a suppression in afferent firing rate. Thus, we see that the peak of afferent activity corresponds to where the electrosensory image is going to be located in the near future, rather than where it is currently located. Thus, the high-pass characteristics of P-type afferent response dynamics give rise to a transformation of the raw electrosensory image which can be viewed as providing a prediction of the future prey location. Such a transformation could aid the animal in generating appropriate motor commands to guide the prey towards the mouth during the post-detection phase of the behavior.

Finally, we speculate that the multiple maps in the brainstem electrosensory nucleus (Heiligenberg and Dye, 1982; Shumway, 1989a,b; Turner et al., 1996) may subserve different stages of prey capture behavior. The lateral map of the electrosensory lateral line lobe (ELL) appears to be ideal for mediating the early stage of prey capture, which requires the detection of a weak electrosensory signal that is distributed over a relatively large area of the receptor surface. Pyramidal cells in the lateral map have larger spatial receptive fields and lower AM thresholds (Shumway, 1989a) and, consequently, should be more sensitive to weak diffuse stimuli than units in other ELL subdivisions. Lateral map units also prefer higher temporal frequencies (Shumway, 1989a; Turner et al., 1996), making them well-suited for detecting the relatively high-frequency AM signals generated during the rapid reverse thrust immediately following prey detection. The centromedial map of the ELL, in contrast, may be better matched to the final stage of prey capture. Pyramidal cells in the centromedial map have smaller spatial receptive fields, which could provide the finer spatial resolution needed to track the prey accurately as it approaches the mouth. Centromedial units also prefer lower AM frequencies, which are characteristic of the final stage of prey capture as the relative velocity between the fish and prey decreases towards zero. Recently, it has been shown that the lateral and centromedial maps of the ELL subserve distinct functions: electrocommunication and jamming avoidance, respectively (Metzner and Juranek, 1997). It will be interesting to discover whether these same maps also subserve functions related to prey detection and localization as suggested above or, alternatively, whether detection and localization might be associated exclusively with the centrolateral map of the ELL, which has spatial and temporal tuning properties intermediate between those of the other two maps.

We would like to thank Noura Sharabash for her skilful assistance in data collection and analysis and the staff of the Beckman Institute Visualization, Media and Imaging Laboratory for their assistance. This research was supported by a grant from the National Institute of Mental Health (R01MH49242).

References

Bastian, J. (1981). Electrolocation. I. How the electroreceptors of *Apteronotus albifrons* code for moving objects and other electrical stimuli. *J. Comp. Physiol.* **144**, 465–479.

Bastian, J. (1986). Electrolocation: behavior, anatomy and physiology. In *Electroreception* (ed. T. H. Bullock and W. Heiligenberg), pp. 577–612. New York: Wiley.

Bastian, J. (1995). Electrolocation. In *The Handbook of Brain Theory and Neural Networks* (ed. M. Arbib), pp. 352–356. Cambridge, MA: MIT Press.

Blake, R. W. (1983). Swimming in the electric eels and knifefishes. *Can. J. Zool.* **61**, 1432–1441.

Carr, C. E., Maler, L. and Sas, E. (1982). Peripheral organization and central projections of the electrosensory nerves in gymnotiform fish. *J. Comp. Neurol.* **211**, 139–153.

Franchina, C. R. and Hopkins, C. D. (1996). The dorsal filament of the weakly electric Apteronotidae (Gymnotiformes; Teleostei) is specialized for electroreception. *Brain Behav. Evol.* **47**, 165–178.

Hagedorn, M. (1986). The ecology, courtship and mating of gymnotiform electric fish. In *Electroreception* (ed. T. H. Bullock and W. Heiligenberg), pp. 497–525. New York: Wiley.

Heiligenberg, W. and Dye, J. (1982). Labeling of electroreceptive afferents in a gymnotoid fish by intracellular injection of horseradish peroxidase: the mystery of multiple maps. *J. Comp. Physiol.* **148**, 287–296.

Hoekstra, D. and Janssen, J. (1986). Lateral line receptivity in the mottled sculpin (*Cottus bairdi*). *Copeia* **1**, 91–96.

Kirk, K. L. (1985). Water flows produced by *Daphnia* and *Diaptomus*: Implications for prey selection by mechanosensory predators. *Limnol Oceanogr.* **30**, 679–686.

Knudsen, E. I. (1975). Spatial aspects of the electric fields generated by weakly electric fish. *J. Comp. Physiol.* **99**, 103–118.

Lannoo, M. J. and Lannoo, S. J. (1993). Why do electric fishes swim backwards? An hypothesis based on gymnotiform foraging behavior interpreted through sensory constraints. *Env. Biol. Fishes* **36**, 157–165.

MacIver, M. A., Lin, J. and Nelson, M. E. (1996). Estimation of signal characteristics during electrolocation from video analysis of prey capture behavior in weakly electric fish. In *Computational Neuroscience: Trends in Research, 1997* (ed. J. M. Bower), pp. 729–734. New York: Plenum Press.

MacIver, M. A. and Nelson, M. E. (1997). Cobalt blocks modulation of ampullary and mechanosensory lateral line units but not tuberous units in the weakly electric fish *Apteronotus leptorhynchus*. *Soc. Neurosci. Abstr.* **23**, 247.

Metzner, W. and Juranek, J. (1997). A sensory brain map for each behavior. *Proc. Natl. Acad. Sci. USA* **94**, 14798–14803.

Montgomery, J. C. (1989). Lateral line detection of planktonic prey. In *The Mechanosensory Lateral Line: Neurobiology and Evolution* (ed. S. Coombs, P. Gorner and H. Munz), pp. 551–574. New York: Springer-Verlag.

Nelson, M. E., Xu, Z. and Payne, J. R. (1997). Characterization and modeling of P-type electrosensory afferent responses to amplitude modulations in a wave-type electric fish. *J. Comp. Physiol.* A **181**, 532–544.

Peters, R. C. and Bretschneider, F. (1972). Electric phenomena in the habitat of the catfish *Ictalurus nebulosus* LeS. *J. Comp. Physiol.* **81**, 345–362.

Rasnow, B. (1996). The effects of simple objects on the electric field of *Apteronotus*. *J. Comp. Physiol.* A **178**, 397–411.

Scheich, H., Bullock, T. H. and Hamstra, R. H. J. (1973). Coding properties of two classes of afferent nerve fibers: high frequency electroreceptors in the electric fish *Eigenmannia*. *J. Neurophysiol.* **36**, 39–60.

Scheich, H., Langner, G., Tidemann, C., Coles, R. B. and Guppy, A. (1986). Electroreception and electrolocation in platypus. *Nature* **319**, 401–402.

Shumway, C. A. (1989a). Multiple electrosensory maps in the medulla of weakly electric gymnotiform fish. I. Physiological differences. *J. Neurosci.* **9**, 4388–4399.

Shumway, C. A. (1989b). Multiple electrosensory maps in the medulla of weakly electric gymnotiform fish. II. Anatomical differences. *J. Neurosci.* **9**, 4400–4415.

Turner, R. W., Plant, J. R. and Maler, L. (1996). Oscillatory and burst discharge across electrosensory topographic maps. *J. Neurophysiol.* **76**, 2364–2382.

von der Emde, G. (1994). Active electrolocation helps *Gnathonemus petersii* to find its prey. *Naturwissenschaften* **81**, 367–369.

von der Emde, G. (1999). Active electrolocation of objects in weakly electric fish. *J. Exp. Biol.* **202**, 1205–1215.

von der Emde, G. and Bleckmann, H. (1998). Finding food: senses involved in foraging for insect larvae in the electric fish *Gnathonemus petersii*. *J. Exp. Biol.* **201**, 969–980.

Wilkens, L. A., Russell, D. F., Pei, X. and Gurgens, C. (1997). The paddlefish rostrum functions as an electrosensory antenna in plankton feeding. *Proc. R. Soc. Lond. B* **264**, 1723–1729.

Winemiller, K. O. and Adite, A. (1997). Convergent evolution of weakly electric fishes from floodplain habitats in Africa and South America. *Env. Biol. Fishes* **49**, 175–186.